

CHEMISTRY

A European Journal

A Journal of



Accepted Article

Title: Facile redox-induced aromatic-antiaromatic interconversion of a β -tetracyano-21,23-dithiaporphyrin under ambient conditions

Authors: Ken-ichi Yamashita, Kana Nakajima, Yusuke Honda, and Takuji Ogawa

This manuscript has been accepted after peer review and appears as an Accepted Article online prior to editing, proofing, and formal publication of the final Version of Record (VoR). This work is currently citable by using the Digital Object Identifier (DOI) given below. The VoR will be published online in Early View as soon as possible and may be different to this Accepted Article as a result of editing. Readers should obtain the VoR from the journal website shown below when it is published to ensure accuracy of information. The authors are responsible for the content of this Accepted Article.

To be cited as: *Chem. Eur. J.* 10.1002/chem.201905823

Link to VoR: <http://dx.doi.org/10.1002/chem.201905823>

Supported by
ACES

WILEY-VCH

FULL PAPER

Facile redox-induced aromatic-antiaromatic interconversion of a β -tetracyano-21,23-dithiaporphyrin under ambient conditions

Ken-ichi Yamashita,* Kana Nakajima, Yusuke Honda, and Takuji Ogawa*

Abstract: Facile redox-induced aromatic-antiaromatic interconversions were accomplished using β -tetracyano-21,23-dithiaporphyrin ($\text{CN}_4\text{S}_2\text{Por}$). Introduced cyano groups not only increased the reduction potential of the porphyrin core but also stabilized the antiaromatic isophlorin ($\text{CN}_4\text{S}_2\text{lph}$) by π -conjugation. The reduction of $\text{CN}_4\text{S}_2\text{Por}$ with hydrazine in polar solvents quantitatively affords $\text{CN}_4\text{S}_2\text{lph}$, even under ambient conditions. $\text{CN}_4\text{S}_2\text{lph}$ retains a nearly planar conformation and exhibits considerable antiaromaticity. Aerobic oxidation of $\text{CN}_4\text{S}_2\text{lph}$ to $\text{CN}_4\text{S}_2\text{Por}$ occurs in nonpolar solvents. This study was conducted to contribute to the understanding of the structure–antiaromaticity relationship.

Introduction

Aromatic-antiaromatic interconversion in cyclic π -conjugated systems attracts growing attention because it changes drastically physical (e.g., magnetic and spectroscopic) properties.^[1] Interconversions have been accomplished by various approaches, the 2e-oxidation/reduction being the most favored one.

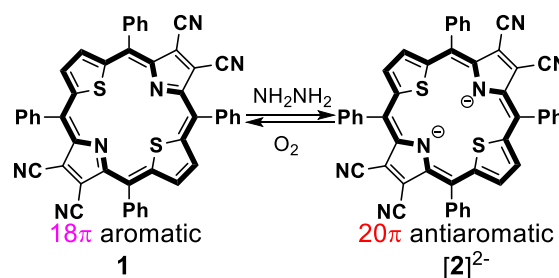
Porphyrinoids, specifically expanded porphyrins, are undoubtedly key compounds in this field and a considerable amount of stable antiaromatic porphyrinoids were synthesized.^[1] Isophlorins are two-electron reduced products of basic porphyrins (18π aromatic), and therefore they potentially have 20π antiaromatic properties.^[2] The basic isophlorins are generally unstable and difficult to isolate.

There are three types of well-characterized isophlorins. One is the deformed isophlorin. Introducing a substituent on their periphery or the internal nitrogen atoms changes their 20π antiaromaticity, improving their stability.^[3–6]

The second type of isophlorins contain tetravalent elements such as Si or Ge^[7–9] or their respective analogues.^[10–13] They complement isophlorins in terms of their charge valance because isophlorins serve as tetravalent ligands. Although these isophlorins are sensitive to oxidation, they can be isolated and their structure, antiaromaticity, and other physical properties have been well-studied. The central metals suppress the deformation of the isophlorin macrocycle and retain their antiaromaticity.

The third type is the core-modified isophlorins. Tetraoxa- and dioxadithiaisophlorin are representatives of stable isophlorins with strong antiaromatic characteristics.^[14] The electron-deficient pentafluorophenyl (C_6F_5 -) substituents at the *meso*-position of those isophlorins contribute to their stabilization. A tetrathia-analogue had nonplanar conformation and therefore nonaromatic properties because of the steric repulsion of the bulky S atoms.^[15,16] Recently, antiaromatic trioxa-analogues were reported and for the first time converted to aromatic porphyrins by 2e-oxidation.^[17] Core-modifications with heteroatoms inhibit π -conjugation and result in destabilization of the oxidized 18π aromatic state.^[2,14,17] Therefore, the synthesis of stable antiaromatic isophlorins with a core-modification number of two or less is not only challenging,^[18] but also important to understand structure-antiaromaticity relationships.

Herein, we report the facile and reversible reduction of a 21,23-dithiaporphyrin derivative to the corresponding antiaromatic isophlorin (Scheme 1). Typically, dithiaporphyrins have low reduction potentials (Table 2), which complicates the synthesis of isophlorins.^[19] To increase the reduction potentials, electron-deficient substituents should be introduced to the peripheral positions of the molecule. Four cyano groups were added to the β -positions of the pyrrole ring of 21,23-dithia-*meso*-tetraphenylporphyrins (S_2TPP) because β -tetracyanotetraphenylporphyrin (CN_4TPP) have significantly higher reduction potentials than unsubstituted TPP.^[20]



Scheme 1. Redox-interconversion between 18π aromatic β -tetracyano- S_2TPP 1, and the reduced 20π antiaromatic isophlorin $[2]^{2-}$.

Results and Discussion

The compound β -tetracyano- S_2TPP 1, which is an oxidized form of isophlorin $[2]^{2-}$, was synthesized for the first time by the copper-catalyzed cyanation of β -tetrabromo- S_2TPP ^[21]. In our hands, however, the synthesis under the same conditions as that of CN_4TPP (i.e., the reaction in pyridine)^[22] was unsuccessful. After changing the solvent to 1,3-dimethyl-2-imidazolinone (DMI), which is more suitable for copper(I)-catalyzed reactions,^[23] the

[*] Dr. K. Yamashita, K. Nakajima, Y. Honda, Prof. Dr. T. Ogawa
Department of Chemistry, Graduate School of Science, Osaka
University, 1-1 Machikaneyama, Toyonaka, Osaka, 560-0043,
Japan
E-mail: yamashita-k@chem.sci.osaka-u.ac.jp,
ogawa@chem.sci.osaka-u.ac.jp

Supporting information for this article is given via a link at the end of the document.

FULL PAPER

desired product **1** was obtained. To increase the product yield, the resultant reaction mixture was treated with aqueous FeCl₃. The observed yields were 30% without and 45% with treatment, respectively. The low yield obtained in the absence of FeCl₃ is probably due to reduction of the product under the reaction conditions (*vide infra*). FeCl₃ oxidizes the reduced species to reproduce **1**.

X-ray diffraction of **1** showed (Figure 1, and Table 1), that the crystal contained two crystallographic independent molecules. One molecule (*molecule A*) had a saddle-shaped conformation while the other (*molecule B*) had a wave-shaped conformation. Values of mean plane deviation, defined by 24 core atoms, are 0.19 (*molecule A*) and 0.11 (*molecule B*), which are similar to that for S₂TPP (0.13).^[24] The harmonic oscillator model of aromaticity (HOMA) indices, which are used as an index for evaluating the degree of bond-length alternation and therefore (anti)aromaticity of cyclic conjugated π systems,^[25,26] were 0.859 and 0.810 for *molecule A* and *B*, respectively. These values are slightly smaller than that for S₂TPP (0.91),^[24] but do not indicate any significant bond-length alternation. According to the DFT calculation (B3LYP/6-31+G**), the optimized structure with the saddle-shaped conformation was slightly more stable than that with the wave-shaped structure (0.41 kcal mol⁻¹). Moreover, the wave-shaped structure had one imaginary frequency as the result of frequency calculation, suggesting the instability of this conformation in the vacuum state.

Table 1. Selected structural data for structure **1** and **[2](PPh₄)₂**.

| | 1 A | 1 B | [2](PPh₄)₂ |
|---|------------|------------|---|
| conformation | saddle | wave | *[c] |
| (C≡N) _{av} / Å | 1.147 | 1.150 | 1.157 |
| (C _β -CN) _{av} / Å | 1.430 | 1.430 | 1.419 |
| (C _{β-pyrrole} =C _{β-pyrrole}) _{av} / Å | 1.364 | 1.357 | 1.424 |
| mpd / Å ^[a] | 0.19 | 0.11 | 0.17 |
| HOMA ^[b] | 0.859 | 0.810 | 0.501 (0.508) |

[a] Mean plane deviation defined by 24 core atoms. [b] Calculated for the circuits representing the bold line shown in Figure 1. The value in parentheses is considered for the whole macrocycle skeleton. [c] See Figure S1.

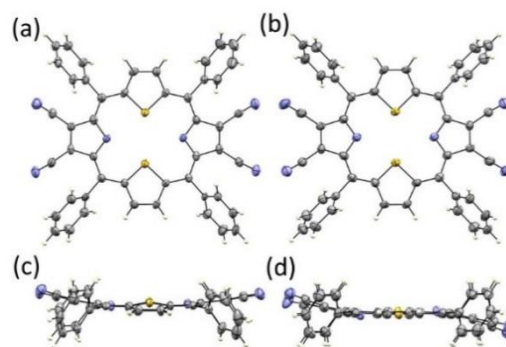


Figure 1. Crystal structures of **1**. Thermal ellipsoid representations (40% probability level) of top (a, and b) and side views (c, and d) for *molecule A* and *molecule B*, respectively. C = gray, H = white, N = blue, and S = yellow. Solvated molecules (CHCl₃) are omitted for clarity.

Physical properties of **1** in nonpolar solvents resembled typical aromatic porphyrins. In the NMR spectrum of **1** in CDCl₃ (Figure 2a), the sharp singlet signal for β protons was observed downfield (9.64 ppm) due to the diatropic ring current in **1** with 18 π aromatic character. The UV/vis absorption spectrum in CH₂Cl₂ exhibited an intense Soret band at 463 nm and split Q bands at longer wavelengths (Figure 3). The Q(0,0) band was observed at 767 nm, which is at a considerably longer wavelength than that of S₂TPP (698 nm).^[27] Moreover, **1** exhibited NIR fluorescence (730–1100 nm) with a peak maximum of 854 nm in CH₂Cl₂ (Figure 3), which is also substantially red-shifted compared to those reported for S₂TPP (λ_{\max} = 706 nm in CHCl₃^[28] and λ_{\max} = 711 nm in CH₂Cl₂^[27]). The fluorescence quantum yield (Φ_f) of **1** was 0.007.

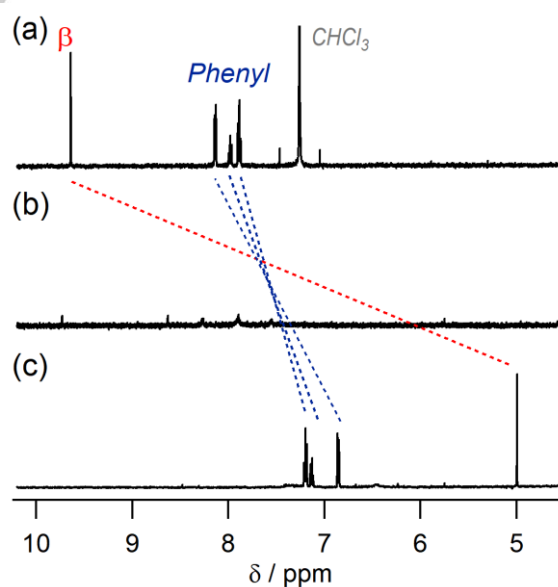


Figure 2. ¹H NMR (500 MHz) spectra of (a) **1** in CDCl₃, (b) in [D₆]DMSO, (c) and **[2]²⁻** generated by the in-situ reduction using NH₂NH₂·H₂O in [D₆]DMSO.

FULL PAPER

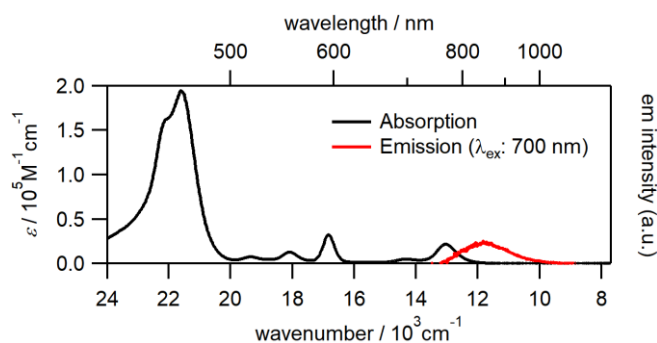


Figure 3. UV/vis/NIR absorption (black) and emission (red) spectra of **1** in CH_2Cl_2 .

The behavior of **1** in highly polar solvents (e.g., DMSO, DMF) is quite different from that in nonpolar solvent described above. ^1H NMR spectra in $[\text{D}_6]\text{DMSO}$ (Figure 2b) or $[\text{D}_7]\text{DMF}$ (Figure S3a), showed that the signal for the β -protons disappeared, and signals for the phenyl rings were significantly broadened. The UV/vis absorption spectrum in DMSO was broadened compared to that in nonpolar solvents, and a new peak appeared at 925 nm (Figure S4). These results suggest that a part of **1** was spontaneously reduced to the anion radical in those solvents. Evidence was definitively provided by ESR measurement of **1** in DMSO, and a distinct peak was observed at $g = 2.00390$ (Figure S5).

Cyclic and differential-pulse voltammetry was performed in both nonpolar and polar solvents (Figure S6), and the observed redox potentials are summarized in Table 2. In CH_2Cl_2 , **1** exhibited two reversible reduction waves at -0.54 and -0.81 V and two oxidation waves at 1.08 and 1.26 V, the latter being irreversible. Those potentials were significantly positive-shifted compared to those of $\text{S}_2\text{TPP}^{[19]}$, as expected. The HOMO-LUMO gap of **1**, estimated by the difference between $E_{\text{ox}1}$ and $E_{\text{red}1}$, was 1.62 eV ($13,100$ cm^{-1}), which was smaller than that of S_2TPP (2.02 eV, $16,300$ cm^{-1}).

On the other hand, in DMSO, those redox potentials were ca. 0.2 V positive-shifted, indicating that reduced states are more stable in polar solvent. In addition, the third reduction peak was observed at -2.19 V.

Table 2. Half-wave potentials (V vs Fc/Fc^+) of **1** and S_2TPP . Potential values of **1** were obtained from differential pulse voltammetry (DPV).

| | solvent | $E_{\text{ox}2}$ | $E_{\text{ox}1}$ | $E_{\text{red}1}$ | $E_{\text{red}2}$ | $E_{\text{red}3}$ |
|------------------------------|--------------------------|------------------|------------------|-------------------|-------------------|-------------------|
| 1 | CH_2Cl_2 | $(1.26)^{[b]}$ | 1.08 | -0.54 | -0.81 | $-^{[c]}$ |
| | DMSO | $-^{[c]}$ | $-^{[c]}$ | -0.33 | -0.61 | -2.19 |
| $\text{S}_2\text{TPP}^{[a]}$ | CH_2Cl_2 | | 0.70 | -1.32 | -1.69 | |

[a] Data from ref 19. [b] Irreversible peak. [c] Out of the potential window.

Due to the markedly positive-shifted reduction potentials, **1** readily underwent $2e^-$ -reduction by weak reducing agent. When **1**

was treated with hydrazine monohydrate in DMSO, the color of the solution changed rapidly from brown to reddish purple. In the UV/vis/NIR spectrum of the product (Figure 4), the intense Soret band of **1** disappeared and three new absorption bands appeared. The longest band was extended to 1050 nm (9500 cm^{-1}) and its molar extinction coefficient (ϵ) was less than 10^3 . These bands are characteristic of the antiaromatic porphyrinoid with a narrow HOMO-LUMO gap and therefore indicated the generation of $[\mathbf{2}]^{2-}$. The second and third absorption bands have a clear vibronic structure. TDDFT calculation of $[\mathbf{2}]^{2-}$ suggested that the first, second, and third absorption band correspond to $\text{S}_0 \rightarrow \text{S}_1$ (HOMO \rightarrow LUMO), $\text{S}_0 \rightarrow \text{S}_2$ (HOMO \rightarrow LUMO+1), and $\text{S}_0 \rightarrow \text{S}_3$ (HOMO-1 \rightarrow LUMO), respectively (Table S6).

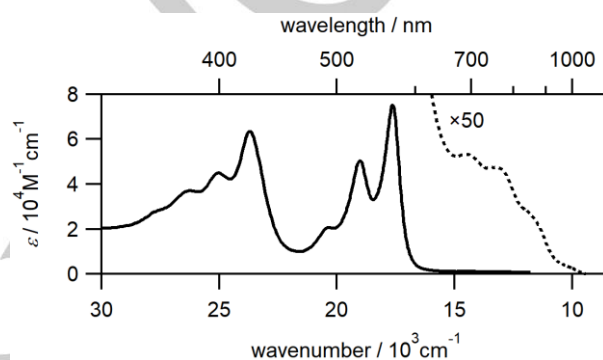


Figure 4. UV/vis/NIR absorption spectra of $[\mathbf{2}]^{2-}$ in DMSO in the presence of $\text{NH}_2\text{NH}_2 \cdot \text{H}_2\text{O}$ (1%). Dashed line was magnified 50 times.

The ^1H NMR spectrum of **1** reduced with $\text{NH}_2\text{NH}_2 \cdot \text{H}_2\text{O}$ in $[\text{D}_6]\text{DMSO}$ indicated the formation of antiaromatic isophlorin $[\mathbf{2}]^{2-}$ as a sole product. The spectrum exhibited a sharp singlet signal for β protons at 4.99 ppm (Figure 3c), which were, compared to **1**, considerably upfield shifted. Comparison of the chemical shifts of selected isophlorins with antiaromatic $^{[7-14,17,18]}$ and nonaromatic $^{[3-6]}$ characters, other relevant antiaromatic porphyrinoids, $^{[29-31]}$ quinoidal thiophene compounds $^{[32,33]}$ is summarized in Table S16. The peak of $[\mathbf{2}]^{2-}$ is shifted downfield compared to those of the strong antiaromatic analogues (from 3 to -1 ppm), but shifted upfield compared to those of the distorted nonaromatic analogues and quinoidal thiophene compounds (from 8 to 6 ppm). Therefore, $[\mathbf{2}]^{2-}$ has moderate antiaromaticity. Similar results were also observed in $[\text{D}_7]\text{DMF}$ (Figure S3b). No signals assignable to NH proton were observed within the range of those for analogous compounds (from 30 to 7 ppm, Figure S7). $^{[3-5,17,18]}$ This indicates that $[\mathbf{2}]^{2-}$ is not protonated in the solution.

To attempt the isolation of $[\mathbf{2}]^{2-}$, the product was extracted with CHCl_3 from DMSO/water solutions of $[\mathbf{2}]^{2-}$. However, the color of the extracted product was brown. The ^1H NMR (Figure S8) and UV/vis (Figure S9) spectra of the obtained compound in halogenated solvents are identical to those of **1**, indicating the aerobic oxidation of $[\mathbf{2}]^{2-}$ to **1**. These results suggest that $[\mathbf{2}]^{2-}$ is stabilized by high-polar solvents. In fact, $[\mathbf{2}]^{2-}$ was not reduced at all with hydrazine in nonpolar solvents but in polar solvent such

For internal use, please do not delete. Submitted_Manuscript

FULL PAPER

as DMF, MeOH, water, and hydrazine, which is consistent with the electrochemical study results.

As-generated product $[2]^{2-}$ (probably a hydrazinium salt) was difficult to isolate due to its high solubility. Therefore, $[2]^{2-}$ was isolated as the less-soluble tetraphenylphosphonium (PPh_4^+) salt, upon adding a methanol solution of PPh_4^+Br to the $[2]^{2-}$ -solution in MeOH, water, or hydrazine to precipitate of $[2](\text{PPh}_4)_2$. Notably, addition of other salts containing tetraalkylammonium or Na(18-crown-5) cation also afforded the precipitate, indicating counter cation exchange. These results also support that $[2]^{2-}$ is not protonated in polar solution. Moreover, slow mixing, following the liquid-liquid layer diffusion method, resulted in single crystals of $[2](\text{PPh}_4)_2$. X-ray diffraction (Figure 5, Table 1) revealed a nearly planar conformation of $[2]^{2-}$ with a small mean plane deviation value (0.17). Compared to **1**, clear bond-alternation was identified in the isophlorin macrocycle, except for the pyrrole rings. The HOMA value obtained from the crystal structure of $[2]^{2-}$ was 0.501, which was considerably smaller than that of **1**. Comparing this value with those of the relevant compounds, it was found to be within the range of typical antiaromatic porphyrinoids, and considerably higher than those of nonaromatic porphyrinoids (Table S16). These data also support the moderate antiaromaticity of $[2]^{2-}$. The average CN bond distances of the introduced cyano groups in $[2]^{2-}$ were slightly elongated compared to those of **1** (Table 1), indicating the decrease in bond order of the cyano groups. This was also supported by IR measurements (Figure S10). A CN stretching peak was shifted by 33 cm^{-1} to lower wavelength upon reduction (2218 and 2185 cm^{-1} for **1** and $[2](\text{PPh}_4)_2$, respectively).

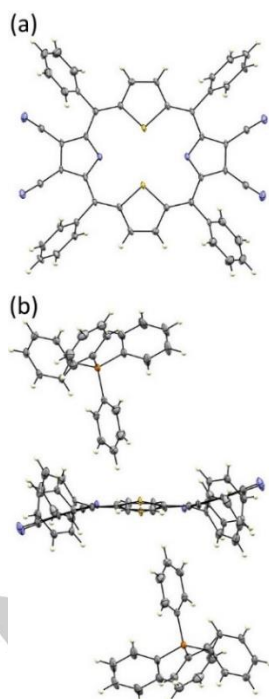


Figure 5. Thermal ellipsoid representations (40% probability level) of the $[2](\text{PPh}_4)_2$ crystal structure. (a) Top view without PPh_4 cation, (b) side view with PPh_4 cation. C = gray, H = white, N = blue, S = yellow, and P = orange.

To obtain further insight into the antiaromaticity of $[2]^{2-}$, we calculated the anisotropy of the induced current density (AICD)^[34] and the nucleus-independent chemical shift (NICS)^[35,36]. The AICD plot revealed the expected counterclockwise ring current for the antiaromatic π -systems (Figure 6). Although both heteroatoms inside $[2]^{2-}$ and β -carbons can contribute to the 20π antiaromatic ring, the ring current indicated that the contribution of $\text{C}_{\beta\text{-pyrrole}}$ was almost negligible, that is, only nitrogen atoms inside the ring contributed. The contribution of $\text{C}_{\beta\text{-thiophene}}$ and thiophene atoms inside the ring were similar.

NICS values for $[2]^{2-}$ were consistent with the AICD result (Tables 3, S7). NICS(0) values of a (center of the macrocycle) and b, which are inside the counterclockwise current, were 6 and 5, respectively, while that of c (center of the pyrrole ring), which was outside the counterclockwise current, was negative (-11.0). The value of d (center of the thiophene ring) was a lower positive value because this point is both inside and outside of the ring currents, as revealed by AICD plots. This might be one of the reasons why the upfield-shift of the β -proton was lower than that of other isophlorin derivatives reported to date.^[2] Notably, the apparently small NICS values near the sulfur atoms (a,b,d, and e) are affected by the considerably strong diamagnetic contribution of the sulfur atoms, supported by each of the components of the chemical shift tensor (Table S7). Therefore, NICS_{zz} values, which are the zz components of the chemical shift tensor and are more reliable indexes for the evaluation of aromaticity, are considerably large (Table 3), thus supporting the antiaromaticity of $[2]^{2-}$.

To consider the effect of the cyano groups on the antiaromaticity, a NICS calculation for an unsubstituted isophlorin $[\text{S}_2\text{lph}]^{2-}$ was performed. All the obtained NICS values were considerably higher than those of $[2]^{2-}$, suggesting that introducing cyano groups decreases the antiaromaticity (Table 3).

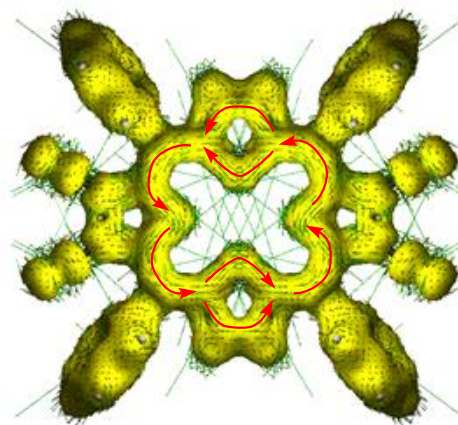
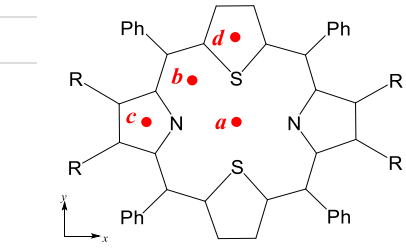


Figure 6. AICD plot for $[2]^{2-}$ (isosurface value: 0.03).

For internal use, please do not delete. Submitted_Manuscript

FULL PAPER

Table 3. NICS (HF/6-311+G**/B3LYP/6-31+G**) values for $[2]^{2-}$ (R = CN) and $[S_2]ph]^{2-}$ (R = H).^[a]

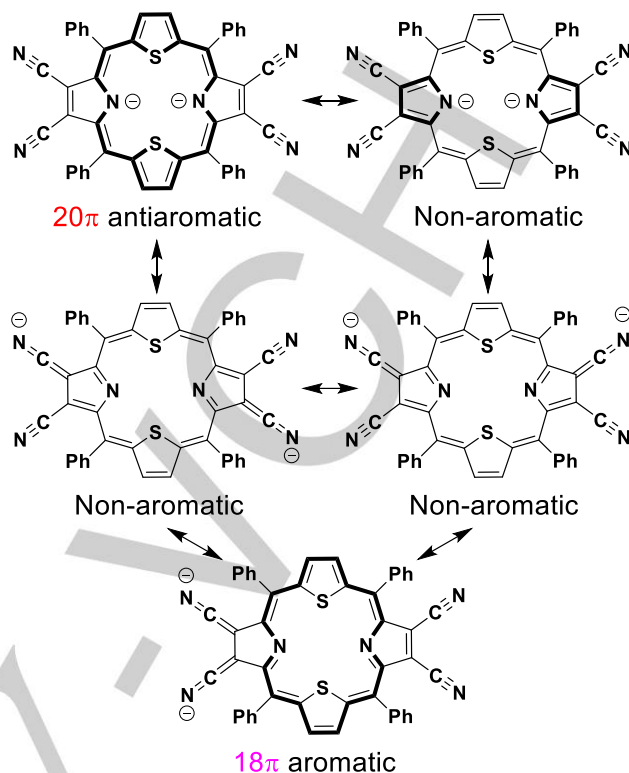


| | a(0) ^[b] | a(1) ^[c] | b ^[b] | c ^[b] | d ^[b] |
|-----------------|---------------------|---------------------|------------------|------------------|------------------|
| $[2]^{2-}$ | 6 (30) | 6 (20) | 5 (38) | -11 (2) | -1 (28) |
| $[S_2]ph]^{2-}$ | 14 (51) | 13 (41) | 15 (68) | -8 (3) | 5 (46) |

[a] NICS_{iso} values are shown. The values in parentheses are NICS_{zz} values.
[b] NICS(0). [c] NICS(1).

Introduction of the four cyano groups increases the number of possible nonaromatic and aromatic resonance structures of $[2]^{2-}$. Therefore, the contribution of the nonaromatic and/or aromatic resonance structure would decrease its antiaromaticity. This was further supported by structural and spectroscopic data; i.e., the elongation of the CN triple bonds and the low-shifts of the CN stretching wavelengths upon reduction. According to the DFT calculations, the negative charge on $[2]^{2-}$ is predominantly located not only on the inner nitrogen atoms (-0.511e) but also on the cyano nitrogen atoms (-0.410e) (Figure S13).

Shinokubo and co-workers reported norcorroles with one or two cyano groups on the β positions.^[37] In this case, effect of the introduced cyano groups on the antiaromaticity is weak compared to our results probably because the introduced cyano groups do not affect the contribution of the possible nonaromatic resonance structures in the norcorrole system.



Scheme 2. Possible resonance structures of $[2]^{2-}$.

Conclusions

The first-time synthesis of β -tetracyanodithiaporphyrin **1** was done, because **1** can easily be reduced to the 20π antiaromatic isophlorin $[2]^{2-}$. Introducing cyano groups into **1** resulted in NIR fluorescence and a high reduction potential in polar solvents. The reversible conversion between **1** and $[2]^{2-}$ was achieved under ambient conditions. Isophlorin $[2]^{2-}$ has a nearly planar conformation and weak antiaromaticity. This is the quite rare examples of 2-core-modified isophlorin with antiaromatic character.^[18] The introduced cyano groups not only stabilized the isophlorins but also weakened its antiaromaticity by π -conjugation within the macrocycle. Because these substituent effects have not been studied extensively before, our results should contribute to the further understanding of the structure-antiaromaticity relationship. Additional research is planned in this regard.

Experimental Section

Instrumentation and Materials

1,3-Dimethyl-2-imidazolidinone (DMI) was distilled from CaH_2 . All other chemicals were of reagent grades and used without any further purification otherwise noted. Analytical thin layer chromatography (TLC) was performed on silica gel 60 F₂₅₄ plates. Column chromatography was performed using silica gel 60N (Kanto Chemical, spherical, neutral, 63–210 μ m). All NMR spectral data were recorded on a JEOL ECA-500 (500

For internal use, please do not delete. Submitted_Manuscript

FULL PAPER

MHz) spectrometer. These data were collected at ambient temperature (25 °C). ¹H NMR spectra were referenced internally to tetramethylsilane as a standard. ¹³C NMR spectra were referenced internally to a solvent signal ($\delta = 77.0, 73.8, \text{ and } 39.5 \text{ ppm}$ for CDCl₃, [D₂]tetrachloroethane, and [D₆]dimethylsulfoxide). ESR spectral data were recorded on a JEOL JES-FA200 spectrometer. ESI HRMS data were measured on a Bruker micrOTOF III. IR measurements were recorded on a JASCO FT/IR-6100 spectrometer equipped with an ATR unit. UV/vis/NIR spectral data were recorded on a Shimadzu UV-3150 spectrometer. Fluorescence spectra were recorded on a HORIBA Fluorolog3-211 spectrometer. The fluorescence quantum yield of **1** was estimated by taking 3,3'-diethyl-5,5-dichloro-3,5-ethylene-4-(diphenylamino)-2,2'-indotricarbocyanine perchlorate (IR-140, Sigma-Aldrich) in ethanol as the standard ($\Phi_f = 0.167$).^[38] Melting points were determined on a Barnstead International MEL-TEMP melting point apparatus. Cyclic and differential pulse voltammetry measurements were carried out using ALS 630E electrochemical analyzer in N₂-saturated CH₂Cl₂ solutions (CH₂Cl₂ or DMSO) containing 0.1 M tetrabutylammonium hexafluorophosphate as a supporting electrolyte at ambient temperature (298 K). A conventional three-electrode cell was used with a glassy carbon working electrode, a platinum wire counter electrode, and a silver wire pseudoreference electrode. Ferrocene was used as the internal standard in all electrochemical experiments, and reported potentials were corrected for Fc/Fc⁺ couple.

Synthesis of 5,10,15,20-tetraphenyl-21,23-dithiaporphyrin

To a solution of 2,5-bis(phenylhydroxymethyl)thiophene^[39] (457 mg, 1.54 mmol) and freshly distilled pyrrole (0.10 mL, 1.4 mmol) in chloroform (135 mL), BF₃·OEt (0.19 mL, 1.5 mmol) was added. The resultant solution was stirred at room temperature under N₂ for 15 h. The resultant solution was added DDQ (257 mg, 1.13 mmol), and then stirred for 30 min. The resultant solution was added triethylamine (0.35 mL), and then concentrated under the reduced pressure. The resultant mixture was dissolved in CHCl₃ and then poured on top of a basic alumina column packed with CHCl₃, then eluted with CHCl₃. The obtained product was further purified by column chromatography (silica gel, hexane/CH₂Cl₂ 1:1), and then recrystallized from CHCl₃-MeOH to give the title compound as a purple solid (72.3 mg, 0.111 mmol, 15%). ¹H NMR spectrum of the product was consistent with that previously reported.^[40]

Synthesis of 7,8,17,18-tetrabromo-5,10,15,20-tetraphenyl-21,23-dithiaporphyrin

To a solution of 5,10,15,20-tetraphenyl-21,23-dithiaporphyrin (120 mg, 0.185 mmol) in chloroform (30 mL), *N*-bromosuccinimide (494 mg, 2.78 mmol) was added. The resultant solution was refluxed for 24 h. After cooling to room temperature, the resultant solution was added triethylamine (2 mL), and then concentrated under the reduced pressure. Then, resultant solution was added the excess of MeOH to precipitate the product. The product was collected by the filtration to give the title compound as a purple solid (157 mg, 0.162 mmol, 93%). ¹H NMR spectrum of the product was consistent with that previously reported.^[21]

Synthesis of 7,8,17,18-tetracyano-5,10,15,20-tetraphenyl-21,23-dithiaporphyrin (1)

7,8,17,18-Tetrabromo-5,10,15,20-tetraphenyl-21,23-dithiaporphyrin (50 mg, 0.052 mmol), CuCN (187 mg, 2.0 mmol) was mixed in freshly distilled DMI (5.4 mL). The resultant mixture was stirred at 150 °C for 48 h under N₂. The resultant mixture was cooled to room temperature, and then added chloroform (13 mL) and a solution of FeCl₃·6H₂O (933 mg) in H₂O (20 mL). The resultant mixture was stirred at 70 °C for 30 min. After cooling to room

temperature, the product was extracted with CHCl₃, and then the organic layer was washed with aqueous NH₃, (x1), water (x1), NH₄Cl aq (x2) and brine (x1), and dried over MgSO₄. Solvent was removed under the reduced pressure. The crude product was purified by column chromatography (silica gel, CH₂Cl₂). Recrystallization from CHCl₃/MeOH gave **1** as a pink purple solid (34 mg, 0.046 mmol, 45%). Analytically pure sample was obtained by recrystallization from CH₂Cl₂/hexane as a purple powder. *R*_f = 0.23 (CH₂Cl₂); m.p.: >300 °C; ¹H NMR (500 MHz, CDCl₃) $\delta = 9.64$ (s, 4H, PorH _{β}), 8.14 (d, *J* = 6.9 Hz, 8H, PhH _{α}), 7.98 (t, *J* = 7.7 Hz, 4H, PhH _{β}), 7.89 (t, *J* = 7.7 Hz, 8H, PhH _{m}); ¹³C NMR (125 MHz, C₂D₂Cl₄) $\delta = 151.4$ (Cq), 149.5 (Cq), 139.6 (CH), 137.5 (Cq), 137.2 (Cq), 133.6 (CH), 130.5 (CH), 128.2 (CH), 124.9 (Cq), 112.0 ppm (Cq); IR (ATR): $\nu = 3055, 3021, 2928, 2218, 1733, 1480, 1444, 1409, 1344, 1263, 1135, 1098, 1053, 1025, 1000, 967, 927, 897, 847, 807, 754, 731, 714, 698, 665, 624, 608, 534, 502, 477 \text{ cm}^{-1}$; UV/Vis (CH₂Cl₂): λ_{max} (Log ϵ) = 451 (sh, 5.20), 463 (5.29), 517 (3.87), 553 (4.10), 594 (4.51), 699 (3.67), 767 nm (4.33); HRMS(ESI): *m/z* calcd for C₄₈H₂₄N₆S₂: 748.1498 (M⁻), found 748.1480; elemental analysis calcd (%) for C₄₈H₂₄N₆S₂: C, 76.99; H, 3.23; N, 11.22; found: C, 76.72; H, 3.20; N, 11.11.

Reduction of **1** and isolation of [2](PPh₄)₂

To a solution of **1** in DMSO or DMF, a few drops of NH₂NH₂·H₂O was added. Color of the solution was rapidly changed to reddish purple. ¹H NMR and UV/vis analyses revealed the quantitative formation of [2]²⁻ probably as a hydrazinium salt.

For the isolation of [2]²⁻, **1** (4.97 mg, 6.63 μmol) was dissolved in NH₂NH₂·H₂O (5 mL). A solution of tetraphenylphosphonium bromide in methanol was gently placed on the top of the resultant solution. After 1 day, microcrystals of [2](PPh₄)₂ was precipitated, collected by the filtration, and dried under vacuum to give [2](PPh₄)₂ as brown microcrystals (5.2 mg, 3.64 μmol , 55%). M.p. (PPh₄ salt): >300 °C; ¹H NMR (hydrazinium salt, 500 MHz, [D₆]DMSO+1%NH₂NH₂·H₂O) $\delta = 7.20$ (t, *J* = 7.3 Hz, 8H, PhH _{m}), 7.13 (t, *J* = 7.3 Hz, 4H, PhH _{β}), 6.86 (d, *J* = 6.9 Hz, 8H, PhH _{α}), 4.99 (s, 4H, PorH _{β}); ¹³C NMR (hydrazinium salt, 125 MHz, [D₆]DMSO+1%NH₂NH₂·H₂O) $\delta = 152.3$ (Cq), 145.6 (Cq), 138.9 (Cq), 131.6 (CH), 129.8 (CH), 128.7 (CH), 127.3 (CH), 126.4 (Cq), 115.6 (Cq), 96.5 ppm (Cq); IR (PPh₄ salt, ATR): $\nu = 3059, 3024, 2921, 2185, 1596, 1584, 1505, 1482, 1435, 1414, 1311, 1143, 1105, 996, 977, 840, 780, 750, 718, 688, 525, 436 \text{ cm}^{-1}$; UV/Vis/NIR (hydrazinium salt, DMSO+1%NH₂NH₂·H₂O): λ_{max} (Log ϵ) = 381 (4.57), 400 (4.65), 422 (4.80), 500 (4.32), 526 (4.70), 567 (4.88) 693 (3.03), 753 (2.98), 860 (sh, 2.70), 970 nm (1.89); elemental analysis (PPh₄ salt) calcd (%) for C₄₈H₂₄N₆S₂P₂·2H₂O: C, 78.78; H, 4.68; N, 5.74; found: C, 78.87; H, 4.63; N, 5.78.

X-Ray crystal structure determinations

Single crystals of **1** suitable for X-ray diffraction study were obtained by slow diffusion of hexane vapor into a solution of **1** in CHCl₃ while those of [2](PPh₄)₂ were obtained by slow diffusion of tetraphenylphosphonium bromide in methanol into a solution of [2]²⁻ (just reduced by NH₂NH₂·H₂O) in methanol. Single-crystal X-ray diffraction data were collected on Rigaku VariMax RAPID FR-E diffractometer, or Rigaku XtaLAB P200 diffractometer using multilayer mirror monochromated Mo-K α radiation ($\lambda = 0.71075 \text{ \AA}$) by the ω scan mode. The crystal was cooled by a stream of cold N₂ gas. Collection, indexing, peak integration, cell refinement, and scaling of the diffraction data were performed using the RAPID AUTO software (Rigaku) or CrystalClear-SM Expert 2.1 b45 software (Rigaku). The data were corrected for Lorentz and polarization effects, and empirical absorption correction was applied. The structures were solved by the SHELXT^[41] program and refined by full-matrix least-squares calculations on *F*² (SHELXL2017)^[42]. All nonhydrogen atoms were modelled

For internal use, please do not delete. Submitted_Manuscript

FULL PAPER

anisotropically. All hydrogen atoms were placed in idealized positions and refined using a riding model [$U_{iso}(H) = 1.2U_{eq}(C)$]. The crystallographic data are summarized in Tables S1 and S2. CCDC 1966841 (**1**), and 1966840 (**2**)[(PPh₄)₂] contain the supplementary crystallographic data for this paper. These data can be obtained free of charge via www.ccdc.cam.ac.uk/data_request/cif.

DFT calculations

All calculations except for AICD were carried out using the Gaussian 16 program package (Revision B.01).^[43] Geometries of all models were optimized by the DFT method at the B3LYP/6-31+G(d,p) level. To confirm that the optimized geometries were not in saddle but in stable points, frequency calculations were performed. The optimized structure of **1** with the saddle-shaped conformation was slightly more stable than that with the wave-shaped structure (0.41 kcal mol⁻¹). Moreover, the wave-shaped structure had one imaginary frequency as the result of frequency calculation, suggesting the instability of this conformation in the vacuum state. Therefore, the saddle-shaped conformation model of **1** was used for the further calculations (e.g., TD-DFT). Charge distribution was calculated by NBO3.

Nucleus-independent chemical shifts (NICS) values were calculated at the GIAO-HF/6-311+G(d,p) level. The anisotropy of the current-induced density (ACID) calculations were performed using the Gaussian 09 program package (Revision E.01)^[44] at the B3LYP/6-31+G(d,p) level using the CSGT method and analyzed using the AICD 2.0.0 program.

Acknowledgements

This work was supported by JSPS KAKENHI Grant Numbers JP17K14447 and JP19H02688. We are grateful to Prof. Rainer Herges (Christian-Albrechts-Universität, Kiel, Germany) for providing the AICD 2.0.0 program. The theoretical calculations were performed using Research Center for Computational Science, Okazaki, Japan.

Conflict of interest

The authors declare no conflict of interest.

Keywords: antiaromaticity • redox chemistry • isophlorin • aromaticity • porphyrinoids

- [1] M. Pawlicki, L. Latos-Grażyński, *Chem. - Asian J.* **2015**, *10*, 1438–1451.
- [2] B. K. Reddy, A. Basavarajappa, M. D. Ambhore, V. G. Anand, *Chem. Rev.* **2017**, *117*, 3420–3443.
- [3] C. Liu, D.-M. Shen, Q.-Y. Chen, *J. Am. Chem. Soc.* **2007**, *129*, 5814–5815.
- [4] X. G. Chen, C. Liu, D. M. Shen, Q. Y. Chen, *Synthesis (Stuttg.)* **2009**, *6*, 3860–3868.
- [5] W. Suzuki, H. Kotani, T. Ishizuka, Y. Shiota, K. Yoshizawa, T. Kojima, *Angew. Chem. Int. Ed.* **2018**, *57*, 1973–1977.
- [6] W. Suzuki, H. Kotani, T. Ishizuka, T. Kojima, *J. Am. Chem. Soc.* **2019**, *141*, 5987–5994.

- [7] J. A. Cissell, T. P. Vaid, A. L. Rheingold, *J. Am. Chem. Soc.* **2005**, *127*, 12212–12213.
- [8] H. E. Song, J. A. Cissell, T. P. Vaid, D. Holten, *J. Phys. Chem. B* **2007**, *111*, 2138–2142.
- [9] J. A. Cissell, T. P. Vaid, G. P. A. Yap, *J. Am. Chem. Soc.* **2007**, *129*, 7841–7847.
- [10] A. Weiss, M. C. Hodgson, P. D. W. Boyd, W. Siebert, P. J. Brothers, *Chem. - Eur. J.* **2007**, *13*, 5982–5993.
- [11] P. J. Brothers, *Inorg. Chem.* **2011**, *50*, 12374–12386.
- [12] T. P. Vaid, *J. Am. Chem. Soc.* **2011**, *133*, 15838–15841.
- [13] J. Conradi, P. J. Brothers, A. Ghosh, *Inorg. Chem.* **2019**, *58*, 4634–4640.
- [14] J. S. Reddy, V. G. Anand, *J. Am. Chem. Soc.* **2008**, *130*, 3718–3719.
- [15] M. Kon-no, J. Mack, N. Kobayashi, M. Suenaga, K. Yoza, T. Shinmyozu, *Chem. - Eur. J.* **2012**, *18*, 13361–13371.
- [16] V. L. Mishra, T. Furuyama, N. Kobayashi, K. Goto, T. Miyazaki, J. S. Yang, T. Shinmyozu, *Chem. - Eur. J.* **2016**, *22*, 9190–9197.
- [17] S. P. Panchal, S. C. Gadekar, V. G. Anand, *Angew. Chem. Int. Ed.* **2016**, *55*, 7797–7800.
- [18] T. Nakabuchi, M. Nakashima, S. Fujishige, H. Nakano, Y. Matano, H. Imahori, *J. Org. Chem.* **2010**, *75*, 375–389.
- [19] A. Ulman, J. Manassen, F. Frolow, D. Rabinovich, *Inorg. Chem.* **1981**, *20*, 1987–1990.
- [20] Y. Terazono, B. O. Patrick, D. H. Dolphin, *Inorg. Chem.* **2002**, *41*, 6703–6710.
- [21] M. Ravikanth, *Chem. Lett.* **2000**, *29*, 480–481.
- [22] P. Bhyrappa, M. Sankar, B. Varghese, *Inorg. Chem.* **2006**, *45*, 4136–4149.
- [23] K.-I. Yamashita, M. Tsuboi, M. S. Asano, K.-I. Sugiura, *Synth. Commun.* **2012**, *42*, 170–175.
- [24] L. Latos-Grażyński, J. Lisowski, L. Szterenber, M. M. Olmstead, A. L. Balch, *J. Org. Chem.* **1991**, *56*, 4043–4045.
- [25] J. Kruszewski, T. M. Krygowski, *Tetrahedron Lett.* **1972**, *13*, 3839–3842.
- [26] T. M. Krygowski, H. Szatyłowicz, O. A. Stasyuk, J. Dominikowska, M. Palusiak, *Chem. Rev.* **2014**, *114*, 6383–6422.
- [27] T. Kaur, W. Z. Lee, M. Ravikanth, *Inorg. Chem.* **2016**, *55*, 5305–5311.
- [28] R. P. Pandian, T. K. Chandrashekar, G. S. S. Saini, A. L. Verma, *J. Chem. Soc. Faraday Trans.* **1993**, *89*, 677–682.
- [29] T. Ito, Y. Hayashi, S. Shimizu, J. Y. Shin, N. Kobayashi, H. Shinokubo, *Angew. Chem. Int. Ed.* **2012**, *51*, 8542–8545.
- [30] T. Satoh, M. Minoura, H. Nakano, K. Furukawa, Y. Matano, *Angew. Chem. Int. Ed.* **2016**, *55*, 2235–2238.
- [31] A. Nishiyama, M. Fukuda, S. Mori, K. Furukawa, H. Fliegl, H. Furuta, S. Shimizu, *Angew. Chem. Int. Ed.* **2018**, *57*, 9728–9733.
- [32] K. Takahashi, T. Suzuki, K. Akiyama, Y. Ikegami, Y. Fukazawa, *J. Am. Chem. Soc.* **1991**, *113*, 4576–4583.
- [33] J. Fujisawa, M. Nagata, M. Hanaya, *Phys. Chem. Chem. Phys.* **2015**, *17*, 27343–27356.
- [34] D. Geuenich, K. Hess, F. Köhler, R. Herges, *Chem. Rev.* **2005**, *105*, 3758–3772.

For internal use, please do not delete. Submitted_Manuscript

FULL PAPER

- [35] P. V. R. Schleyer, C. Maerker, A. Dransfeld, H. Jiao, N. J. R. van Eikema Hommes, *J. Am. Chem. Soc.* **1996**, *118*, 6317–6318.
- [36] C. Corminboeuf, P. von R. Schleyer, R. Puchta, C. S. Wannere, Z. Chen, *Chem. Rev.* **2005**, *105*, 3842–3888.
- [37] R. Nozawa, K. Yamamoto, J.-Y. Shin, S. Hiroto, H. Shinokubo, *Angew. Chem. Int. Ed.* **2015**, *54*, 8454–8457.
- [38] K. Rurack, M. Spieles, *Anal. Chem.* **2011**, *83*, 1232–1242.
- [39] H. J. Xu, J. MacK, D. Wu, Z. L. Xue, A. B. Descalzo, K. Rurack, N. Kobayashi, Z. Shen, *Chem. - Eur. J.* **2012**, *18*, 16844–16867.
- [40] C. E. Stilts, M. I. Nelen, D. G. Hilmey, S. R. Davies, S. O. Gollnick, A. R. Oseroff, S. L. Gibson, R. Hilf, M. R. Detty, *J. Med. Chem.* **2000**, *43*, 2403–2410.
- [41] G. M. Sheldrick, *Acta Crystallogr. Sect. A Found. Adv.* **2015**, *71*, 3–8.
- [42] G. M. Sheldrick, *Acta Crystallogr. Sect. C Struct. Chem.* **2015**, *71*, 3–8.
- [43] M. J. Frisch, G. W. Trucks, H. B. Schlegel, G. E. Scuseria, M. A. Robb, J. R. Cheeseman, G. Scalmani, V. Barone, G. A. Petersson, H. Nakatsuji, X. Li, M. Caricato, A. V. Marenich, J. Bloino, B. G. Janesko, R. Gomperts, B. Mennucci, H. P. Hratchian, J. V. Ortiz, A. F. Izmaylov, J. L. Sonnenberg, D. Williams-Young, F. Ding, F. Lipparini, F. Egidi, J. Goings, B. Peng, A. Petrone, T. Henderson, D. Ranasinghe, V. G. Zakrzewski, J. Gao, N. Rega, G. Zheng, W. Liang, M. Hada, M. Ehara, K. Toyota, R. Fukuda, J. Hasegawa, M. Ishida, T. Nakajima, Y. Honda, O. Kitao, H. Nakai, T. Vreven, K. Throssell, J. Montgomery, J. A., J. E. Peralta, F. Ogliaro, M. J. Bearpark, J. J. Heyd, E. N. Brothers, K. N. Kudin, V. N. Staroverov, T. A. Keith, R. Kobayashi, J. Normand, K. Raghavachari, A. P. Rendell, J. C. Burant, S. S. Iyengar, J. Tomasi, M. Cossi, J. M. Millam, M. Klene, C. Adamo, R. Cammi, J. W. Ochterski, R. L. Martin, K. Morokuma, O. Farkas, J. B. Foresman, D. J. Fox, *Gaussian 16, Rev. B.01, Gaussian, Inc., Wallingford CT 2016*.
- [44] M. J. Frisch, G. W. Trucks, H. B. Schlegel, G. E. Scuseria, M. A. Robb, J. R. Cheeseman, G. Scalmani, V. Barone, B. Mennucci, G. A. Petersson, H. Nakatsuji, M. Caricato, X. Li, H. P. Hratchian, A. F. Izmaylov, J. Bloino, G. Zheng, J. L. Sonnenberg, M. Hada, M. Ehara, K. Toyota, R. Fukuda, J. Hasegawa, M. Ishida, T. Nakajima, Y. Honda, O. Kitao, H. Nakai, T. Vreven, J. A. Montgomery, J. E. Peralta, F. Ogliaro, M. Bearpark, J. J. Heyd, E. Brothers, K. N. Kudin, V. N. Staroverov, R. Kobayashi, J. Normand, K. Raghavachari, A. Rendell, J. C. Burant, S. S. Iyengar, J. Tomasi, M. Cossi, N. Rega, J. M. Millam, M. Klene, J. E. Knox, J. B. Cross, V. Bakken, C. Adamo, J. Jaramillo, R. Gomperts, R. E. Stratmann, O. Yazyev, A. J. Austin, R. Cammi, C. Pomelli, J. W. Ochterski, R. L. Martin, K. Morokuma, V. G. Zakrzewski, G. A. Voth, P. Salvador, J. J. Dannenberg, S. Dapprich, A. D. Daniels, Farkas, J. B. Foresman, J. V. Ortiz, J. Cioslowski, D. J. Fox, *Gaussian 09, Rev. E.01, Gaussian, Inc., Wallingford CT 2009*.

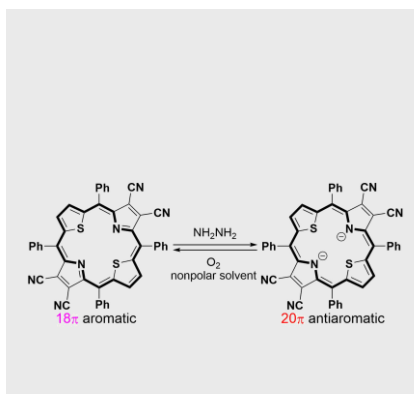
FULL PAPER

Entry for the Table of Contents (Please choose one layout)

Layout 1:

FULL PAPER

Facile redox-induced aromatic-antiaromatic interconversion were accomplished with β -tetracyano-21,23-dithiaporphyrin (CN₄S₂Por). The introduced cyano groups increased not only the reduction potentials of the porphyrin core, but also stabilized the antiaromatic state of isophlorin (CN₄S₂lph) by conjugation.



Ken-ichi Yamashita*, Kana Nakajima,
Yusuke Honda, Takuji Ogawa*

Page No. – Page No.

**Facile redox-induced aromatic-
antiaromatic interconversion of a β -
tetracyano-21,23-dithiaporphyrin
under ambient conditions**